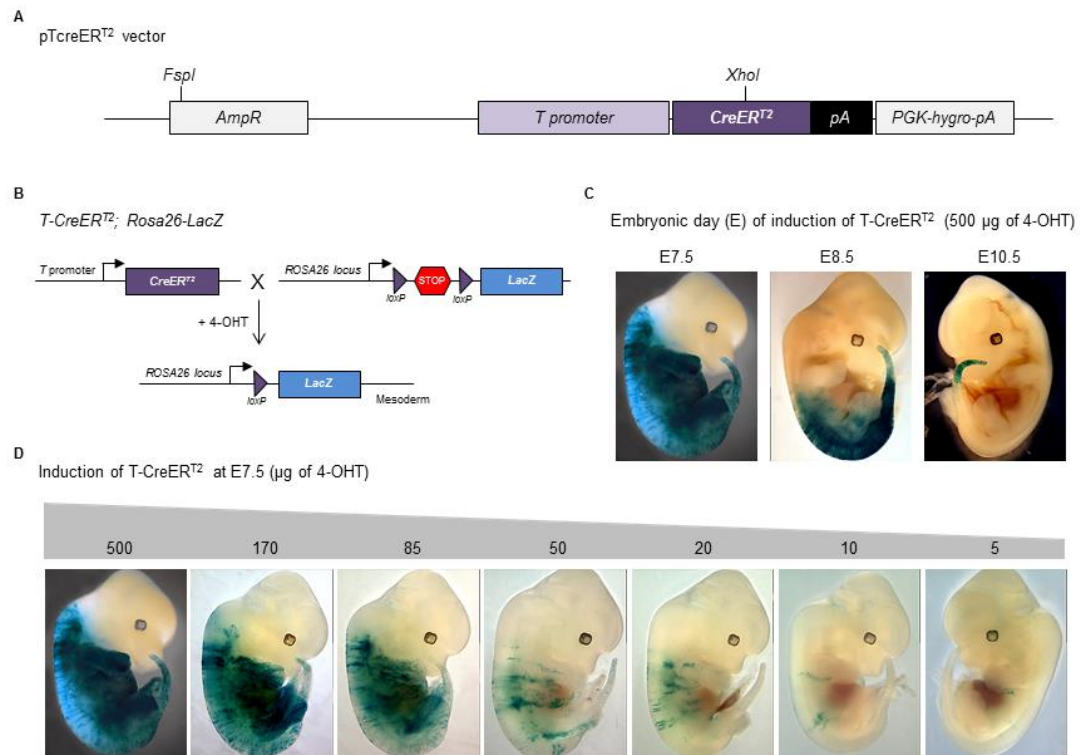**Supplementary Material**

Figure S1

Figure S1. Cre-mediated mosaic recombination in the *T-CreER^{T2}* mouse line. (**A**) Schematic representation of the pTcreER^{T2} transgene used for the generation of the *T-CreER^{T2}* mouse line. (**B**) Cre-mediated recombination of the *Rosa26-lacZ* reporter inducing β-gal activity. (**C**) Whole-mount images of E12.5 *T-CreER^{T2};Rosa26-lacZ* embryos, stained for β-gal after 4-OHT administration at E7.5, E8.5 or E10.5. (**D**) Same as in (C) but after 4-OHT administration at E7.5 with different doses of 4-OHT (5 to 500 µg).
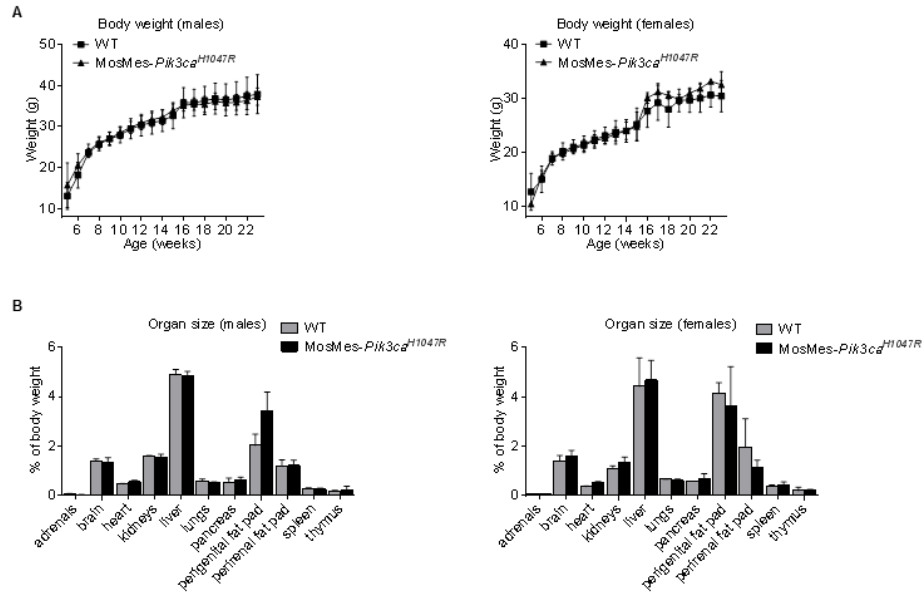
Figure S2

Figure S2. Body weight over time (**A**) and organ size at 6-month-old (**B**) of WT and MosMes-*Pik3ca*^{H1047R} mice. Data represent mean ± SEM, n=30/genotype for (A), n=6/genotype for (B).
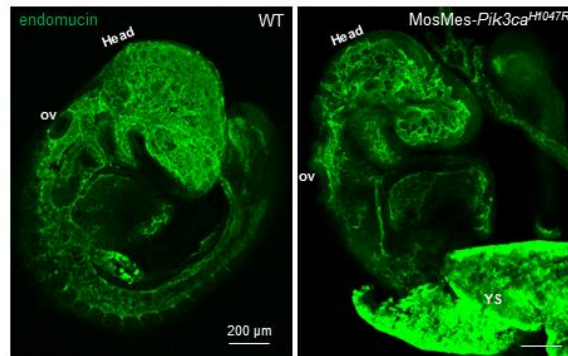
Figure S3

Figure S3. Whole-mount endomucin-stained E9.5 embryos dosed with 170 µg 4-OHT at E7.5. The MosMes-*Pik3ca^{H1047R}* embryo shows an overall less developed vasculature compared to the WT embryo. H, head; ov, otic vesicle; YS, yolk sac.
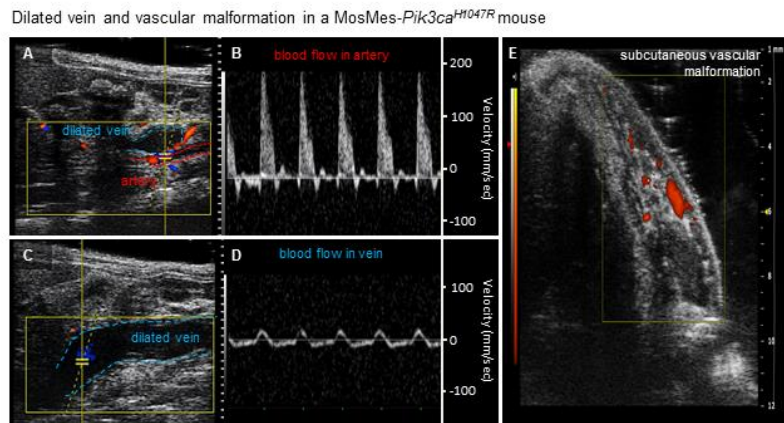
Figure S4

Figure S4. MosMes-*Pik3ca^{H1047R}* mouse with a subcutaneous vascular malformation and dilated vein. (**A,C**) Ultrasound images with colour Doppler showing artery (red dotted line) and dilated vein (blue) of a Yellow markers indicate the region from which pulsed wave Doppler was acquired. (**B,D**) Pulsed wave Doppler measurement of blood flow demonstrates a high arterial flow velocity wave form within the artery (B), and a slow venous flow velocity wave form within the dilated vein (D). (**E**) Power Doppler ultrasound demonstrates slow flow signals in subcutaneous vascular malformation.
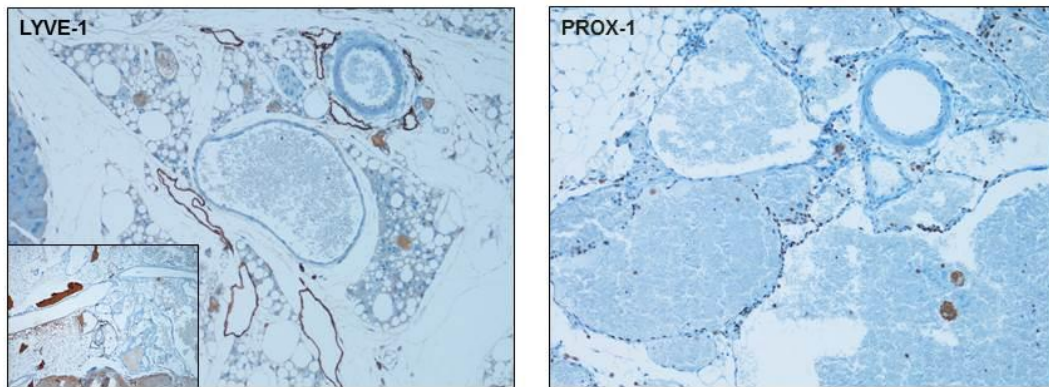
Figure S5

Figure S5. Representative images of immunostaining for lymphatic markers (LYVE-1, PROX-1) in VMs of MosMes-*Pik3ca^{H1047R}* mice. **Left**, LYVE-1 immunostaining, original magnification x100 (x40, inner square). **Right**, PROX-1 immunostaining, original magnification x100.
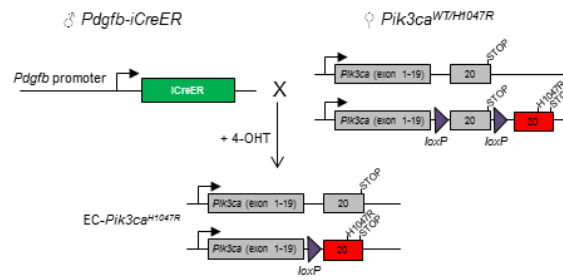
Figure S6

Figure S6. Genetic strategy to activate *Pik3ca^H1047R* in ECs. *Pdgfb-iCreER* mice were crossed with *Pik3ca^WT/H1047R* mice.
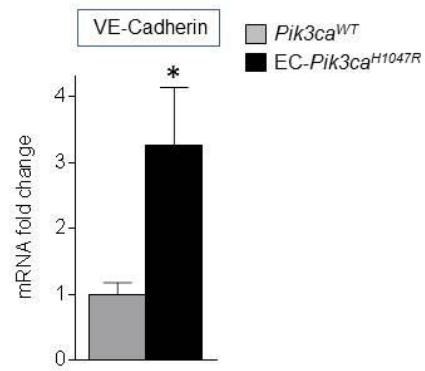
Figure S7

Figure S7. Expression of VE-Cadherin in P6 EC-*Pik3ca^{H1047R}* retinas. VE-Cadherin mRNA expression was normalized to *Hprt*. Data represent mean ± SEM. (Mann-Whitney U test) *p < 0.05. n=5/genotype.

Figure S8

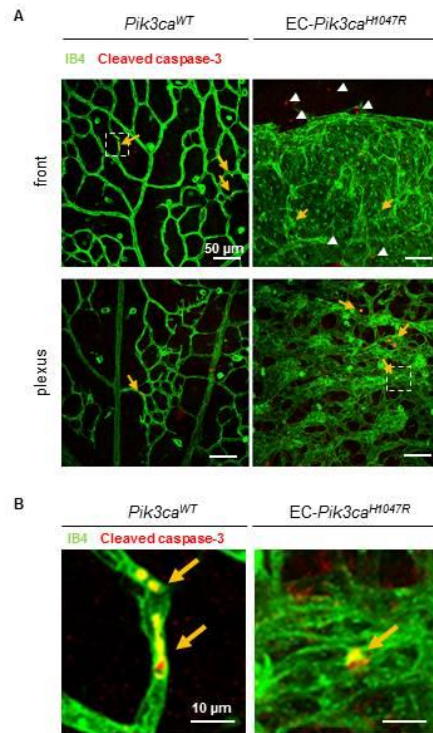**Figure S8.** Apoptosis in P9 EC-*Pik3ca^H1047R^* retinas. (A) Representative flat-mounted *Pik3ca^WT^* and EC-*Pik3ca^H1047R^* P9 retinas, stained with IB4 (green, revealing ECs) and with antibody to cleaved caspase-3 (marker of apoptosis; red). Indicated are apoptotic ECs (orange arrows) and non-EC apoptotic cells (white arrowheads). (**B**) Higher magnification of sections highlighted in (A).
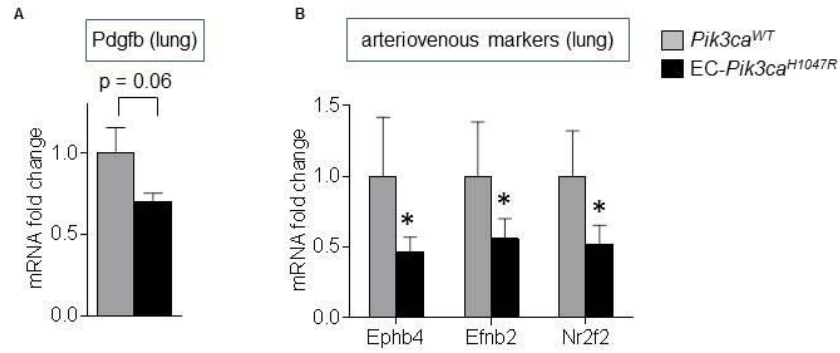
Figure S9

Figure S9. (**A**) Expression of Pdgfb in EC-*Pik3ca*^{H1047R} lungs. Data represent mean ± SEM. (Mann-Whitney U test). (**B**) Expression of Ephb4, Nr2f2 and Efnb2 mRNA in lung lysates of *Pik3ca*^{WT} and EC-*Pik3ca*^{H1047R} P6 mice. Data represent mean ± SEM. *p < 0.05 (Mann-Whitney U test). n=5/genotype.
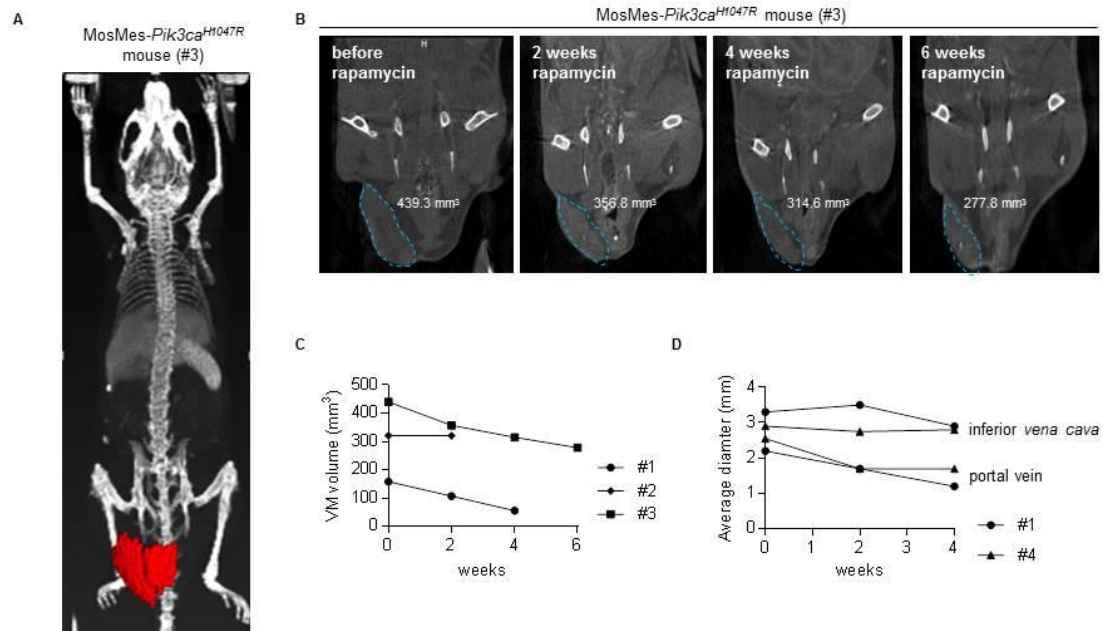
Figure S10

Figure S10. Treatment of MosMes-*Pik3ca^{H1047R}* mice with rapamycin. (**A**) 3D image reconstruction of CT-A of MosMes-*Pik3ca^{H1047R}* mouse #3 before treatment, subcutaneous VM highlighted in red. (**B**) CT-A images MosMes-*Pik3ca^{H1047R}* mouse #3 upon rapamycin treatment showing the volume of the subcutaneous VM (circled in blue). (**C**) Graph showing volumes of VM from MosMes-*Pik3ca^{H1047R}* mice during rapamycin treatment. (D) Graph showing average diameter of inferior *vena cava* and portal vein of MosMes-*Pik3ca^{H1047R}* mice during rapamycin treatment.

Supplementary Table 1. List of organs and tissues subjected to histological examination

(H&E staining) in WT and MosMes-*Pik3ca*^{H1047R} mice

Adrenals	Ovaries/oviducts
Aorta	Pancreas
Brain	Parathyroids
Caecum	Prostate
Cervix	Rectum
Colon	Salivary gland
Duodenum	Seminal vesicles
Epididymis	Skeletal muscle
Eyes	Skin
Perigenital fat pad	Spleen
Perirenal fat pad	Sternum
Femur	Stomach
Heart	Submandibular lymph nodes
Ileum	Testes
Jejunum	Thymus
Kidneys	Thyroids
Liver	Tongue
Lungs	Trachea
Mammary glands	Urinary bladder
Oesophagus	Uterus/vagina

Supplementary Table 2. Percentage of MosMes-*Pik3ca^{H1047R}* mice with VMs after dosing pregnant females with different doses of 4-OHT

μg 4-OHT administered per pregnant mouse	MosMes-*Pik3ca^{H1047R}* mice with VMs
12.5	12.5%
50	15%
250	100%

Supplementary Table 3. Percentage of live WT and MosMes-*Pik3ca^{H1047R}* offspring obtained after administration of different doses of 4-OHT to pregnant females. The expected normal Mendelian distribution is 50% of each genotype.

	observed frequency	
μg 4-OHT administered per pregnant mouse	WT	MosMes-*Pik3ca^{H1047R}*
12.5	50.0%	50.0%
50	48.7%	51.3%
250	61.5%	38.5%